Proceedings of the
44th IEEE Conference on Decision and Control, and
the European Control Conference 2005
Seville, Spain, December 12-15, 2005

Two-Dimensional Frequency Analysis of Structured Uncertainty for Multiple Array Paper Machine Cross-Directional Processes

Junqiang Fan and Guy A. Dumont

Abstract— **This paper provides a two-dimensional frequency analysis technique for robust controllers of large-scale multiple array paper machine cross-directional (CD) processes with structured model uncertainty. For such spatially-distributed dynamical systems, the process model and its realistic structured uncertainty are assumed to be linear, spatially-invariant, and time-invariant. These large-scale MIMO systems are rectangular circulant matrix blocks that can be conveniently transformed into a family of small dimension transfer functions in the two-dimensional frequency domain. This significantly simplifies the controller design and gives a better physical insight about the realistic structured uncertainty problem. Given a linear feedback controller, we can easily derive the robust stability condition for the closed-loop CD system in the two-dimensional frequency domain.**

I. Introduction

This paper considers the model uncertainty issue related to industrial paper machine cross-directional (CD) control systems. Fig. 1 shows a typical paper machine configuration with CD actuator arrays and scanning sensors. Traditional CD control uses pairing rules to choose one actuator array for controlling one paper property while neglecting the interaction of multiple array CD processes. Recently, the simultaneous control of multiple paper sheet properties using multiple actuator arrays has become possible and is gaining wide applications in industry [1].

The objective of a CD control system is usually to maintain the measured CD profiles of paper properties (basis weight, moisture and caliper) as flat as possible. The number of actuators in a typical CD actuator array ranges from 50 to 300 and the sensor reads measurements from 300 to 2000 locations across the sheet. Most well-designed single array CD systems are unfortunately ill-conditioned [2]–[6] even at steady-state. Directionality of multiple array systems introduces another source of ill-conditioning [7]. The large dimensionality and the ill-conditioning make these processes challenging to control.

An industrial CD process model is usually identified using input-output data from a bump test [8]. There inevitably exists model uncertainty due to neglected interaction of multiple array processes, sheet wandering or shifting in the CD, unknown disturbances, actuator's nonlinearity, operation condition changing, nonlinear shrinkage etc.

This work was supported by Honeywell, the Natural Sciences and Engineering Research Council of Canada, and Technology Partnerships Canada.

J. Fan is with Honeywell Automation and Control Solutions, 500 Brooksbank Ave, North Vancouver, BC V7J 3S4, Canada, james.fan@honeywell.com

G. A. Dumont is with Department of Electrical and Computer Engineering, University of British Columbia, Vancouver, BC V6T 1Z4, Canada, guyd@ece.ubc.ca

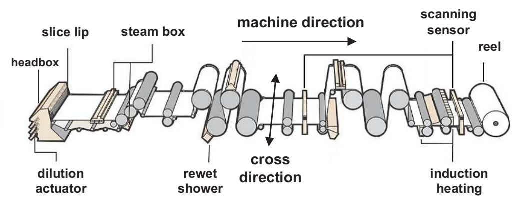

Fig. 1. Wide view of the paper machine showing typical positions of the various actuator arrays and scanning sensor(s).

The CD process model uncertainty is considered as unstructured uncertainty in [6]. These unstructured uncertainty descriptions may include uncertainties which do not exist in real CD processes. In practice, CD model uncertainty may be highly structured [4], [9], [10]. In [4], the authors addressed the parameter uncertainty for both dynamical response and spatial response. In [10], the process model is described by rational transfer functions of spatial and dynamical Laplace variables and includes a structured uncertainty representation. In [5], [11], uncertain pseudo-singular values are considered as model uncertainty. In [9], a frequency method is used to show that a misaligned mapping between the actuators and the measurements results in a narrower achievable closed-loop bandwidth.

In [12], singular value decomposition (SVD) is used to decouple systems where the directionality is independent of frequency into nominally independent subsystems of lower dimensions, and robust analysis based on the structured singular value$-\mu$ is used for these SVD controllers. In [13], symmetric circulant plants (such as squared single array CD systems) and block circulant symmetric systems are decoupled by real Fourier matrices into a series of subsystems. As mentioned in [14], most single array CD systems have much larger dimensions of outputs (measurements) than inputs (actuator numbers). As shown in [14], they can be described by rectangular circulant matrices. Although the pseudo-SVD method of [5], [12] can be used for rectangular single array CD processes, the pseudo-singular values are not directly linked to spatial frequencies, which are familiar in industrial CD control. As for multiple CD array systems, they are neither block circulant symmetric systems [13] nor systems where the directionality is independent of frequency [5], [12].

This paper uses a realistic structured uncertainty based on a model identified by commercial identification software [8]. The multiple array CD process model and its structured un-

0-7803-9568-9/05/$20.00 ©2005 IEEE

certainty can be approximated as time-invariant and spatially-invariant rectangular circulant matrix [14] blocks, and thus be easily transferred from the temporal and spatial domains into the temporal frequency and spatial frequency domains. The structured uncertainty in the two-dimensional frequency domain is then easily understood. If a linear feedback controller such as one in [14] is given, the robust stability condition for the closed-loop system can be derived in the two-dimensional frequency domain. This paper demonstrates that practical considerations for structured uncertainty in real plants eliminate unnecessary conservativeness of a robust controller based on unstructured uncertainty.

The main contribution of this paper is to derive conditions for robust stability of the paper machine model with multiple arrays of sensors and actuators in the face of structured uncertainty.

II. Problem Statement

A. Nominal multiple array CD process model

The process model for a multiple array CD system[1] is defined as follows,

$$\begin{aligned} Y(z) &= G(z)U(z)+D(z), && (1)\\ G(z) &= \begin{bmatrix} G_{11}(z) & G_{12}(z) \\ G_{21}(z) & G_{22}(z) \end{bmatrix}, && (2)\\ G_{ij} &= B_{ij}h_{ij}(z),\ i=1,2,\ j=1,2, && (3) \end{aligned}$$

where $Y(z)=[y_1(z),y_2(z)]^T \in \mathbb{C}^{2m\times 1},\ y_i(z)\in\mathbb{C}^m$,
$U(z)=[u_1(z),u_2(z)]^T \in \mathbb{C}^{(n_1+n_2)\times 1},\ u_j(z)\in\mathbb{C}^{n_j}$,
$D(z)=[d_1(z),d_2(z)]^T \in \mathbb{C}^{2m\times 1},\ d_i(z)\in\mathbb{C}^m$,
$h_{ij}(z)=\frac{z^{-q_{ij}}}{1-a_{ij}z^{-1}},\quad i=1,2,\ j=1,2,$

y_i, u_j, and d_i are $\mathscr{Z}$-transforms of the i^{th} measurement profile, j^{th} actuator setpoint profile, and i^{th} disturbance profile respectively; $B_{ij}\in\mathbb{R}^{m\times n_j}$ is the ij^{th} subplant's spatial response matrix, and $h_{ij}(z)$ is the $\mathscr{Z}$-transform of the ij^{th} subplant's temporal response; n_j with $j=1,2$ is the j^{th} actuator array number, m is the dimension of each controlled property.

The spatial interaction matrix B_{ij} has the following given structure [8],

$$\begin{aligned} B_{ij} &= [b_1,b_2,\cdots,b_{n_j}]\in\mathbb{R}^{m\times n_j}, && (4)\\ b_l &= f(k,\gamma_l,\alpha_l,\xi_l,\beta_l,c_l) && (5)\\ &= \frac{\gamma_l}{2}\big(e^{-\alpha_l(k-c_l+\beta_l\xi_l)^2/\xi_l^2}\cos\left(\pi(k-c_l+\beta_l\xi_l)/\xi_l\right)\\ &\quad +e^{-\alpha_l(k-c_l-\beta_l\xi_l)^2/\xi_l^2}\cos\left(\pi(k-c_l-\beta_l\xi_l)/\xi_l\right)\big),\\ &\quad k=1,\cdots,m,\quad l=1,\cdots,n_j, && (6) \end{aligned}$$

where the gain (γ_l), attenuation (α_l), width (ξ_l), and divergence (β_l) parameters are scalar parameters used for describing the spatial response shape for each actuator, the alignment parameter c_l is the coordinate of the spatial response center for the l^{th} actuator, k is the measurement location. Like most other published CD models, in this work, our model imposes $\gamma_l=\gamma$, $\alpha_l=\alpha$, $\xi_l=\xi$, and $\beta_l=\beta$ for all l. This assumption is based on more than 100 models identified from real paper machines.

[1]Without losing any generality, we use a 2-actuator-array and 2-measurement-array CD system as a representative example.

As we mentioned in the previous section, generally speaking, the multiple array CD process model $G(z)$ in (2) *cannot* be decoupled to $U\Sigma_G(z)V^H$ by SVD as in [5], [12]. Except for special cases and contrary to the single array situation, the multiple array CD process model $G(z)$ cannot be split into two parts: one spatial response part and one temporal response part. As the subplant $G_{ij}(z)$ is not a circulant symmetric matrix, $G(z)$ is neither a block circulant symmetric matrix [13], [15] nor a circulant block matrix [15]. But it does have a special structure which will be explored in Section III.

B. Model uncertainty in industrial CD control

1) Physical motivation: An important class of process model uncertainties that plague the CD process can be characterized as global changes in the process model. In other words, deviations in the process model that influence the response of all actuators simultaneously. There are a variety of mechanisms for this and we present an overview of the main types here.

- Sheet wander, corresponding to a change in the alignment parameter c_l in (6).
- The base loading of an actuator array can alter the cross-directional spatial response shape.
- Paper machine operators will sometimes speed up or slow down the paper machine for production reasons.
- The overall slice opening is sometimes changed to improve the formation of the paper sheet. This action has a drastic impact on the spatial response of the weight profile to the slice lip actuators.
- A common form of global uncertainty is in terms of neglecting the multivariable characteristics of the paper machine. For example, the slice lip illustrated in Fig. 1 is typically used to control the basis weight profile of the paper sheet. The effect on the moisture profile by slice lip actuators has rarely been quantified and almost never incorporated in the control strategy.

There exist other forms of non-global model uncertainty that will affect individual actuators such as:

- Faults such as failure or partial failure of one or more actuators in an array.
- Due to the physical construction of the paper machine, the paper sheet will typically respond differently to the CD actuators near the sheet edges that in the middle of the sheet.
- As water is removed from the drying paper sheet, it may shrink in the CD resulting in the paper sheet being narrower at the scanning sensor than it was at the actuator array.

2) Mathematical model of uncertainty: It is true that no modelling technique can accurately capture all features of an industrial paper machine. Our structured model uncertainty described in the following paragraphs addresses the effects of the *global uncertainty* described above. As for non-global

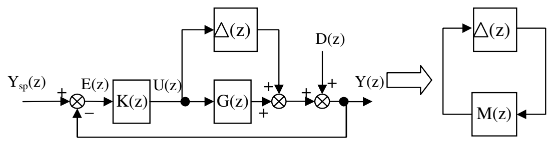

Fig. 2. The linear feedback control system configuration with additive uncertainty, and $M\Delta$ structure used for robust stability analysis.

uncertainty, they may be considered as unstructured model uncertainty.

Generally speaking, for CD processes, correctly addressing model uncertainty in the spatial response shape is crucial due to the ill-conditioned nature of B_{ij} in (4). So in this paper, we just consider spatial uncertainty in the process model,

$$\begin{aligned}
G_p(z) &= G(z)+\Delta(z) \in \mathbb{C}^{2m\times(n_1+n_2)}, && (7)\\
\Delta(z) &= \begin{bmatrix} \Delta_{11}(z) & \Delta_{12}(z) \\ \Delta_{21}(z) & \Delta_{22}(z) \end{bmatrix}, && (8)\\
\Delta_{ij}(z) &= G_{ijp}(z)-G_{ij}(z), && (9)\\
G_{ijp}(z) &= B_{ijp}\cdot h_{ij}(z), && (10)\\
B_{ijp} &= [b_{1p}, b_{2p}, \cdots, b_{n_jp}], && (11)\\
b_{lp} &= f(k,\gamma_p,\alpha_p,\xi_p,\beta_p,c_p), && (12)\\
l &= 1,\cdots,n_j,\ k=1,\cdots,m,
\end{aligned}$$

where $f(\cdot)$ is defined in (5), and each parameter has its own multiplicative uncertainty.

It is difficult to use the standard μ-analysis approach to handle the parameter uncertainties in (12) in the $M\Delta$ structure in Fig. 2 due to the nonlinearity of b_l in (6) and the large dimensionality of the inputs and the outputs in the spatial response matrix B_{ijp} in (11). Therefore, we use the additive structured uncertainty $\Delta_{ij}(z)$ in (9) to replace the parameter uncertainties. The reason is that this structured uncertainty $\Delta_{ij}(z)$ has a special structure – an approximate rectangular circulant matrix [14], which can be easily analyzed in the two-dimensional frequency domain, and will be explored in Section IV-A.

C. Closed-loop system requirements

While applicable to a broad class of practical controllers, the intended application of the results of this work is in the analysis of an industrial model predictive control (MPC) strategy described in [1]. Other literature about CD-MPC may be found in [16]–[22]. Using the technique in [23], [24], we can derive the equivalent transfer matrix $K(z)$ for a multiple array system. Fig. 2 shows a block diagram of such a system. The closed-loop transfer function from the output disturbance $D(z)$ to the error profile $E(z)$ between the target profile $Y_{sp}(z)$ and the measurements $Y(z)$ in Fig. 2 represents the output disturbance attenuation and can be written as,

$$T_{ed}(z) = (I+G(z)K(z))^{-1}, \qquad (13)$$

where $T_{ed}(z) \in \mathbb{C}^{2m\times 2m}$ is also called the output sensitivity function [25].

For the additive model uncertainty $\Delta(z)$ in (8) , the robust stability (RS) of the closed-loop system with a stable loop transfer function $M\Delta$ in Fig. 2 is guaranteed by satisfying the following condition [25], [26],

$$\bar{\sigma}(M(e^{i\omega})\Delta(e^{i\omega})) < 1,\ \forall\omega, \qquad (14)$$

where $\bar{\sigma}$ denotes the maximum singular value, $\Delta(z)$ in (8) is a stable transfer matrix perturbing the nominal model, $M(z)$ is the transfer matrix between the output disturbance $D(z)$ and the actuator profile $U(z)$,

$$T_{ud}(z) = -K(z)(I+G(z)K(z))^{-1}, \qquad (15)$$

where $T_{ud}(z) \in \mathbb{C}^{(n_1+n_2)\times 2m}$ is also called the control sensitivity function.

As CD control is mainly a regulation problem with only occasional setpoint changes, disturbance rejection may be considered as the performance criterion. For CD control systems, given a linear controller $K(z)$ as in Fig. 2, the most important closed-loop requirements are

1) Disturbance rejection, i.e., evaluating the sensitivity matrix $T_{ed}(z)$ in (13) for disturbance attenuation;
2) Robust stability, i.e., making the controller $K(z)$ in Fig. 2 stabilizing for the set of plants $G_p(z)$ in (7).

III. Two-Dimensional Frequency Analysis

In this section, we simply summarize some of the work presented in [14], where a technique was introduced that allows the process models such as $G_{ij}(z)$ in (2) to be approximated as spatially invariant using rectangular circulant matrices. This allows subsequent decoupling of the single array CD process models in the two-dimensional frequency domain. Then this technique is generalized to multiple array systems such as $G(z)$ in (1) by pre- and post- multiplication of Fourier matrices and unitary permutation matrices [7].

It is known that these single CD arrays systems $G_{ij(z)}$ are spatially bandlimited [27]. Therefore, $G_{ij}(z)$ in (2) are approximated as spatially bandlimited RCMs [14]. Let $\widetilde{G}_{ij}(z)(=F_mG_{ij}(z)F_{n_j}^H)$ represent the model in the spatial frequency domain, where $F_m \in \mathbb{C}^{m\times m}$ and $F_{n_j} \in \mathbb{C}^{n_j\times n_j}$ are the complex Fourier matrices. Note that $\widetilde{G}_{ij} \in \mathbb{C}^{m\times n_j}$ has the diagonal nonzero elements as illustrated in Fig. 3, which represent spatial frequency gains, due to its RCM characteristic [14]. In Fig. 3, $g_{ij}(\nu_0,z)$ is the gain at zero spatial frequency, $g_{ij}(\nu_k,z)$ and $\widetilde{g}_{ij}(\nu_k,z)$ are conjugate and represent the same spatial frequency gain with different phases, $p=q-1=$

$$\widetilde{G}_{ij}(z) = \left[\begin{array}{cccc:cccc}
g_{ij}(\nu_0,z) & & & & 0 & & & \\
& g_{ij}(\nu_1,z) & & & & 0 & & \\
& & \ddots & & & & \ddots & \\
& & & g_{ij}(\nu_p,z) & & & & 0 \\
\hdashline
0 & & & & 0 & & & \\
& 0 & & & & 0 & & \\
& & \ddots & & & & \ddots & \\
& & & 0 & & & & 0 \\
\hdashline
0 & & & & \widetilde{g}_{ij}(\nu_q,z) & & & \\
& 0 & & & & \widetilde{g}_{ij}(\nu_{q-1},z) & & \\
& & \ddots & & & & \ddots & \\
& & & 0 & & & & \widetilde{g}_{ij}(\nu_1,z)
\end{array}\right]$$

Fig. 3. Diagonal property of the subplant model $\widetilde{G}_{ij}(z)$ in the spatial frequency domain.

$$\widehat{\mathbf{G}}(z) = \left[\begin{array}{ccccccc} g(\nu_0,z) & & & & & & \\ & g(\nu_1,z) & & & & & \\ & & \widetilde{g}(\nu_1,z) & & & & \\ & & & \ddots & & & \\ & & & & g(\nu_k,z) & & \\ & & & & & \widetilde{g}(\nu_k,z) & \\ & & & & & & \ddots \\ \hline 0 & & & \cdots & & & 0 \\ \vdots & & & \ddots & & & \vdots \\ 0 & & & \cdots & & & 0 \end{array}\right] \begin{array}{l} \left.\begin{array}{l} \\ \\ \\ \\ \\ \\ \\ \end{array}\right\} \widehat{\mathbf{G}}_1(z) \\ \\ \\ \\ \end{array}$$

Fig. 4. Block diagonal property of $\widehat{G}(z)$ in (16).

$n_j/2-1$ for even n_j, and $p = q-1 = (n_j-1)/2$ for odd n_j, where n_j is the number of columns of $\widetilde{G}_{ij}$.

The multiple array CD process model in the two-dimensional frequency domain can be obtained through

$$\widehat{G}(z) = P_y \mathbf{F}_y G(z) \mathbf{F}_u^H P_u^T, \tag{16}$$

where $P_y \in \mathbb{R}^{2m\times 2m}$ and $P_u \in \mathbb{R}^{(n_1+n_2)\times(n_1+n_2)}$ are(unitary) permutation matrices, and $\mathbf{F}_y$ and $\mathbf{F}_u$ are

$$\mathbf{F}_y = \begin{bmatrix} F_m & 0 \\ 0 & F_m \end{bmatrix}, \ \mathbf{F}_u = \begin{bmatrix} F_{n_1} & 0 \\ 0 & F_{n_2} \end{bmatrix}. \tag{17}$$

The matrix $\widehat{G}(z)$ is illustrated in Fig. 4, where $g(\nu_k,z)$ and $\widetilde{g}(\nu_k,z)$ are obtained through

$$g(\nu_k,z) = \begin{bmatrix} g_{11}(\nu_k,z) & g_{12}(\nu_k,z) \\ g_{21}(\nu_k,z) & g_{22}(\nu_k,z) \end{bmatrix}, \tag{18}$$

$$\widetilde{g}(\nu_k,z) = \begin{bmatrix} \widetilde{g}_{11}(\nu_k,z) & \widetilde{g}_{12}(\nu_k,z) \\ \widetilde{g}_{21}(\nu_k,z) & \widetilde{g}_{22}(\nu_k,z) \end{bmatrix}. \tag{19}$$

The singular values of $\widehat{G}(z)$ can be obtained through solving the singular values of the small dimension matrices $g(\nu_0,z)$, $g(\nu_k,z)$, and $\widetilde{g}(\nu_k,z)$ which are sorted through spatial frequencies from low to high. Finally we can obtain the singular values of $G(z)$ in (2) according to spatial frequencies.

From [14], [23], for single array systems, if the nominal plant $G_{ij}(z)$ in (2) is a spatially bandlimited RCM, then the unconstrained MPC controller $K(z) \in \mathbb{C}^{n_j\times m}$ in Fig. 2, the sensitivity function $T_{ed}(z) \in \mathbb{C}^{m\times m}$ in (13), and the transfer matrix $T_{ud}(z) \in \mathbb{C}^{n_j\times m}$ in (15) also have a spatially bandlimited RCM structure. Similarly, for multiple array systems, if the nominal plant $G(z)$ in (2) is an RCM-blocks matrix and its subplants $G_{ij}(z)$ are spatially bandlimited, then the unconstrained MPC controller $K(z) \in \mathbb{C}^{(n_1+n_2)\times 2m}$ in Fig. 2, the sensitivity function $T_{ed}(z) \in \mathbb{C}^{2m\times 2m}$ in (13), and the transfer matrix $T_{ud}(z) \in \mathbb{C}^{(n_1+n_2)\times 2m}$ in (15) also have a spatially bandlimited RCM-blocks structure.

IV. Structured Uncertainty and Robust Stability

Transforming the closed-loop transfer matrix $T_{ud}(z)$ in (15) and the structured model uncertainty $\Delta(z)$ in (8) into the two-dimensional frequency domain makes it easy to apply a structured uncertainty analysis to the robust stability (RS) condition (14).

A. Structured uncertainty in the two-dimensional frequency domain

Since $G_{ij}(z)$ in (2) is a spatially bandlimited RCM for any selection of parameters γ etc. in (5), then all $G_{ijp}(z)$ in (10) are spatially bandlimited RCMs for any choice of perturbations. Since the set of all RCMs is closed under summation [14], then $\Delta_{ij}(z)$ in (9) is also a spatially bandlimited RCM. Therefore, from the previous section, the structured uncertainty $\Delta(z) \in \mathbb{C}^{2m\times(n_1+n_2)}$ in (8) has a two-dimensional frequency representation $\delta(\nu_k,z)$ and its singular values can be obtained as follows,

$$\{\delta(\nu_0,z),\cdots,\delta(\nu_{k_{\max}},z)\} = diag(P_y F_y \Delta(z) F_u^H P_u^T), \tag{20}$$

$$\sigma_j(\Delta(z)) = [\Sigma(\delta(\nu_0,z)),\Sigma(\delta(\nu_1,z)),\cdots, \Sigma(\delta(\nu_{k_{\max}},z))],\ j=1,\cdots,n_1+n_2, \tag{21}$$

where $\Sigma(\delta)$ denotes the singular values of δ.

For instance, if the nominal parameters[2] in (6) of the single array plant model $G_{ij}(z)$ in (3) have uncertainty limits $\delta_1 = 0.25$ and $\delta_2 = 0.6$ in (12), the additive structured model uncertainty $\Delta_{ij}(z)$ can be calculated from (9). Fig. 5 shows the nominal steady-state spatial responses to a single actuator and the responses with parameter uncertainties in the spatial domain. Fig. 6 illustrates the corresponding perturbations $\delta(\nu_j,z)|_{z=1}$ in (20) in the spatial frequency domain. For single array systems, $\overline{\sigma}_j(\Delta(z)) = |\delta(\nu_j,z)|$.

Note the figures show only the structured uncertainty at dynamical steady-state ($\omega = 0$) in the spatial frequency domain for clear display. In Figs. 5a-e, only one parameter has uncertainty, while Fig. 5f shows a class of response shapes combining uncertainty in all parameters. Similarly, Figs. 6a-e illustrate the effect of uncertainty in one parameter as indicated in order to separate each parameter's contributions to the total structured model uncertainty. Fig. 6f shows a class of structured model uncertainties which include uncertainty in all the parameters in the spatial frequency domain. The dashed line may be considered as the maximum uncertainty limit across the spatial frequencies at steady-state. The non-global model uncertainty mentioned in Section II-B.1 cannot be transferred into the spatial frequency domain as it is not an RCM. However, if its singular values are under the dashed curve along the spatial frequencies in Fig. 6f, then the next subsection's robust stability condition for structured uncertainty still holds for these non-global uncertainties.

Generally speaking, it is always possible to diagonalize $\Delta_{ij}(z)$ in (9) at each dynamical frequency using the singular value decomposition (SVD) as in [11], [12]. However, it is difficult to directly relate singular vectors to physical variables, such as spatial frequencies. When the RCM structure of $\Delta_{ij}(z)$ in (9) is exploited then its singular vectors can be given by the harmonic functions of the spatial variable [6], [14].

A casual analysis of Fig. 6 indicates that uncertainty in the selected model parameters has its strongest effect at

[2]The nominal parameters in (6) are $\gamma = 0.00647$, $\alpha = 1.2$, $\xi = 10$, $\beta = 0.10$, $c_i = 2.5 + 5(i-1)$ for $i = 1,\cdots,64$, $m = 320$, $n_1 = 64$.

the mid-range spatial frequencies. While it is not unusual to find systems with low uncertainty at low frequencies, these plots should not be interpreted to indicate that high spatial frequencies are easily controllable. On the contrary, the relatively low model uncertainty simply indicates that we are relatively certain that the process model gain is small at high spatial frequencies. For the same percentage of model uncertainty, the divergence and alignment parameter are two most sensitive parameters compared to the gain, width, and attenuation parameters.

B. Robust stability for multiple array systems

As mentioned above, for a multiple array system, the control sensitivity function $T_{ud}(z)$ is an RCM-blocks matrix which can be decoupled into a sequence of small dimension MIMO transfer functions and whose singular values can be solved as follows,

$$\{t_{ud}(\nu_0,z),\cdots,t_{ud}(\nu_{k_{\max}},z)\} = diag(P_uF_uT_{ud}(z)F_y^HP_y^T), \quad (22)$$

$$\sigma_j(T_{ud}(z)) = [\Sigma(t_{ud}(\nu_0,z)),\Sigma(t_{ud}(\nu_1,z)),\cdots, \Sigma(t_{ud}(\nu_{k_{\max}},z))],\ j=1,\cdots,n_1+n_2. \quad (23)$$

For unstructured additive uncertainty, the RS condition [25], [26] in (14) can be rewritten for stable $T_{ud}(z)$ and $\Delta(z)$ as,

$$\max_j \left(\overline{\sigma}(t_{ud}(\nu_j,e^{i\omega}))\right) < \frac{1}{\overline{\sigma}(\Delta(e^{i\omega}))}, \quad \forall\omega, \quad (24)$$

However, if the perturbation $\Delta(z)$ is structured as in (8), then, the RS condition (24) is conservative. In this case, $\Delta(z)$ is an RCM-blocks matrix, the RS condition in (14) can be expressed in the tighter form,

$$\begin{aligned}&\overline{\sigma}(T_{ud}(e^{i\omega})\Delta(e^{i\omega}))\\ &= \overline{\sigma}\left((P_uF_uT_{ud}(e^{i\omega})F_y^HP_y^T)\cdot(P_yF_y\Delta(e^{i\omega})F_u^HP_u^T)\right)\\ &= \max_j(\overline{\sigma}(t_{ud}(\nu_j,e^{i\omega})\cdot\delta(\nu_j,e^{i\omega}))) < 1,\ \forall\ \omega, \quad (25)\end{aligned}$$

where F_y, F_u, P_y, and P_u are from (17) and (16) respectively, $\nu_j \in \{\nu_0,\nu_1,\cdots,\nu_{k_{max}}\}$ in (21) and $\omega \in [0,\omega_N]$ with the dynamical Nyquist frequency ω_N. In the above derivation, we used the fact that F_y, F_u, P_y, and P_u are unitary matrices, and that singular values are invariant under similarity transformations.

Note that for structured uncertainties the RS condition (25) is less conservative than (24) as it takes directionality into account. The unstructured RS condition (24) is equivalent to

$$\max_j(\overline{\sigma}(t_{ud}(\nu_j,e^{i\omega})))\max_k(\overline{\sigma}(\delta(\nu_k,e^{i\omega}))) < 1,\forall\omega, \quad (26)$$

which can be significantly worse than (25) since it "pairs-up" the two maxima. Fig. 7 demonstrates the conservativeness of the controller based on unstructured uncertainties for a single array system. Note that for single array systems, $\sigma(t_{ud}(\nu_j,1)) = |t_{ud}(\nu_j,1)|$, $\sigma(\delta(\nu_j,1)) = |\delta(\nu_j,1)|$. Note that Fig. 7 only shows the steady-state $\omega=0$ case for clear display.

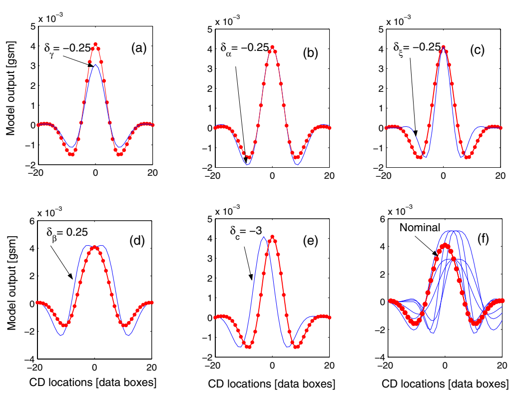

Fig. 5. The nominal spatial response b_i in (4) (solid+dotted line) and its corresponding one with uncertainty b_{ip} in (11) (solid line): (a) the gain γ_p, (b) the attenuation α_p, (c) the width ξ_p, and (d) the divergence β_p in (12) have -25% parameter uncertainty respectively; (e) the alignment parameter c has 60% actuator spacing uncertainty in (12); (f) mixing all the parameters uncertainty together.

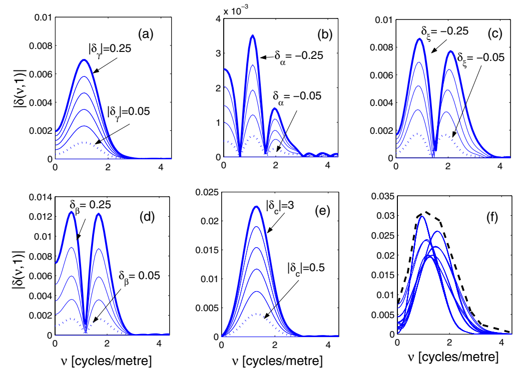

Fig. 6. The additive structured uncertainty $|\delta(\nu_j,e^{i\omega}|$ (for a single array system) in (20) for $\omega=0$ in the spatial frequency domain due to: (a) the gain γ_p has -25% to 25% uncertainty; (b) the attenuation α_p and (c) the width ξ_p both have -25% to 0% uncertainty; (d) the divergence β_p has 0% to 25% uncertainty; (e) the alignment c has -60% to 60% actuator spacing uncertainty; (f) mixing all the parameters' uncertainty.

V. Industrial Example

An industrial example of structured uncertainty will be presented in this section. This example will show that the changing of actuator operating position has a drastic impact on the spatial response.

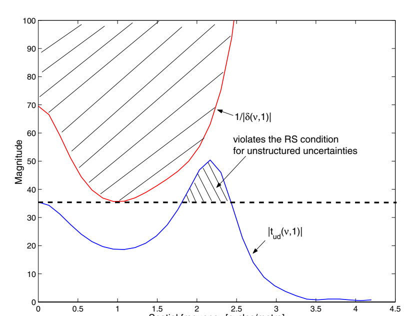

Fig. 7. An example shows that the controller may satisfy the RS condition (25) for structured uncertainties but violates the RS condition (26) for unstructured uncertainty in a single array CD system.

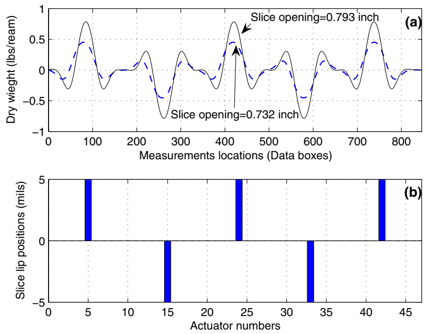

Fig. 8. Dry weight response changing due to different overall slice openings: (a) modelled dry weight spatial responses due to moving slice lip actuators as shown in (b); (b) the slice lip actuator profile.

The identified models are from a real working paper machine in the USA. This paper machine uses slice lip actuators (actuator number $n_1 = 47$) to control dry weight profile (measurement data boxes $m = 846$). Fig. 8 shows the dry weight spatial responses to slice lip actuators for two different overall slice openings. As mentioned in Section II-B.1, changing the overall slice opening results in drastic change of the dry weight spatial response to slice lip actuators. In this example, the slice lip opening is changed from 0.732 *inch* to 0.793 *inch*, but the dry weight spatial response parameters in (6) to slice lip actuators are changed as follows,

$$\begin{aligned} \gamma &= 0.1811 \rightarrow 0.2772,\ \alpha = 1.5 \rightarrow 1.2, \\ \xi &= 45.567 \rightarrow 38.275,\ \beta = 0.3 \rightarrow 0.3. \end{aligned}$$

Although the overall slice opening is only changed about 8.3%, the gain parameter is changed about 53%.

VI. Conclusions

This article has presented a technique for analyzing robust controllers for paper machine CD processes with multiple sensors and actuator arrays in face of structured uncertainty. This technique is based on a realistic structured model uncertainty for industrial CD processes and extends the robust controller analysis and design methods for traditional dynamical systems into the two-dimensional frequency domain.

This approach allows analysis of the real CD process model uncertainty in the spatial frequency domain, and provides a better physical insight into the role of the model uncertainty. Robust stability conditions for multiple array systems with structured uncertainty are derived as a simple formula in the two-dimensional frequency domain.

References

[1] J. U. Backström, C. Gheorghe, G. E. Stewart, and R. Vyse, "Constrained model predictive control for cross directional multi-array processes," *Pulp & Paper Canada*, vol. 102, no. 5, pp. T128–T131, May 2001.

[2] W. P. Heath, "Orthogonal functions for cross-directional control of web forming processes," *Automatica*, vol. 32, no. 2, pp. 183–198, 1996.

[3] K. Kristinsson and G. A. Dumont, "Cross-directional control on paper machines using Gram polynomials," *Automatica*, vol. 32, no. 4, pp. 533–548, 1996.

[4] D. Laughlin, M. Morari, and R. D. Braatz, "Robust performance of cross-directional control systems for web forming processes," *Automatica*, vol. 29, no. 6, pp. 1395–1410, 1993.

[5] A. P. Featherstone, J. G. VanAntwerp, and R. D. Braatz, *Identification and Control of Sheet and Film Processes*. Springer, 2000.

[6] G. E. Stewart, D. M. Gorinevsky, and G. A. Dumont, "Feedback controller design for a spatially-distributed system: The paper machine problem," *IEEE Transactions on Control Systems Technology*, vol. 11, no. 5, pp. 612–628, September 2003.

[7] J. Fan and G. E. Stewart, "Fundamental spatial performance limitation analysis of multiple array paper machine cross-directional processes," in *Proc. the American Control Conference 2005*, Portland, Oregon, USA, June 2005, pp. 3643–3649.

[8] D. M. Gorinevsky and C. Gheorghe, "Identification tool for cross-directional processes," *IEEE Transactions on Control Systems Technology*, vol. 11, no. 5, pp. 629–640, September 2003.

[9] S. Gendron and J. Hamel, "On paper streaks caused by mapping misalignment of the cross-direction control system," in *Control Systems 2002*, Stockholm, Sweden, 2002, pp. 117–122.

[10] D. M. Gorinevsky and G. Stein, "Structured uncertainty analysis of spatially distributed paper machine process control," in *Proc. the American Control Conference*, Arlington, VA, USA, 2001, pp. 2225–2230.

[11] J. G. VanAntwerp, A. P. Featherstone, and R. D. Braatz, "Robust cross-directional control of large scale sheet and film processes," *Journal of Process Control*, vol. 11, pp. 149–177, 2001.

[12] M. Hovd, R. D. Braatz, and S. Skogestad, "SVD controllers for H_2-, H_∞- and μ-optimal control," *Automatica*, vol. 33, no. 3, pp. 433–439, 1997.

[13] M. Hovd and S. Skogestad, "Control of symmetrically interconnected plants," *Automatica*, vol. 30, no. 6, pp. 957–973, 1994.

[14] J. Fan, G. E. Stewart, and G. A. Dumont, "Two-dimensional frequency analysis for unconstrained model predictive control of cross-directional processes," *Automatica*, vol. 40, no. 11, pp. 1891–1903, 2004.

[15] P. J. Davis, *Circulant Matrices (2nd Edition)*. Chelsea Publishing, 1994.

[16] J. G. VanAntwerp and R. D. Braatz, "Fast model predictive control of sheet and film processes," *IEEE Transactions on Control Systems Technology*, vol. 8, no. 3, pp. 408–417, May 2000.

[17] A. Rigopoulos, "Application of principal component analysis in the identification and control of sheet-forming processes," Ph.D. dissertation, Georgia Institute of Technology, USA, 1999.

[18] D. R. Saffer II, F. J. Doyle III, A. Rigopoulos, and P. Wisnewski, "MPC study for a dual headbox CD control problem," in *Proc. Control Systems 2000*, Victoria, BC, Canada, May 2000, pp. 97–100.

[19] J. C. Campbell, J. B. Rawlings, and C. V. Rao, "Efficient implementation of model predictive control for sheet and film forming processes," *AICHE Journal*, vol. 44, no. 8, pp. 1713–1723, 1998.

[20] J. Fan, G. E. Stewart, and G. A. Dumont, "Model predictive cross-directional control using a reduced model," in *Proc. Control Systems 2002*, Stockholm, Sweden, June 2002, pp. 65–69.

[21] B. Haznedar and Y. Arkun, "Single and multiple property CD control of sheet forming processes via reduced order infinite horizon MPC algorithm," *Journal of Process Control*, vol. 12, no. 1, pp. 175–192, January 2002.

[22] R. Bartlett, L. Biegler, J. Backstrom, and V. Gopal, "Quadratic programming algorithms for large-scale model predictive control," *Journal of Process Control*, vol. 12, pp. 775–795, 2002.

[23] J. Fan, "Model predictive control for multiple cross-directional processes: Analysis, tuning, and implementation," Ph.D. dissertation, The University of British Columbia, Vancouver, Canada, 2003. [Online]. Available: http://ahousat.library.ubc.ca/theses/available/etd-07142004-143355/

[24] J. M. Maciejowski, *Predictive Control with Constraints*. Pearson Education, 2001.

[25] S. Skogestad and I. Postlethwaite, *Multivariable Feedback Control: Analysis and Design*. John Wiley & Sons, Inc., 1996.

[26] K. Zhou, J. C. Doyle, and K. Glover, *Robust and optimal control*. Prentice Hall, Inc., 1996.

[27] S. R. Duncan and G. F. Bryant, "The spatial bandwidth of cross-directional control systems for web processes," *Automatica*, vol. 33, no. 2, pp. 139–153, February 1997.